Clinical Cancer Research

PEST Domain Mutations in Notch Receptors Comprise an Oncogenic Driver Segment in Triple-Negative Breast Cancer Sensitive to a γ-Secretase Inhibitor

Kai Wang[1], Qin Zhang[1], Danan Li[1], Keith Ching[1], Cathy Zhang[1], Xianxian Zheng[1], Mark Ozeck[1], Stephanie Shi[2], Xiaorong Li[1], Hui Wang[1], Paul Rejto[1], James Christensen[1], and Peter Olson[1]

Abstract

Purpose: To identify and characterize novel, activating mutations in Notch receptors in breast cancer and to determine response to the gamma secretase inhibitor (GSI) PF-03084014.

Experimental Design: We used several computational approaches, including novel algorithms, to analyze next-generation sequencing data and related omic datasets from The Cancer Genome Atlas (TCGA) breast cancer cohort. Patient-derived xenograft (PDX) models were sequenced, and Notch-mutant models were treated with PF-03084014. Gene-expression and functional analyses were performed to study the mechanism of activation through mutation and inhibition by PF-03084014.

Results: We identified mutations within and upstream of the PEST domains of NOTCH1, NOTCH2, and NOTCH3 in the TCGA dataset. Mutations occurred via several genetic mechanisms and compromised the function of the PEST domain, a negative regulatory domain commonly mutated in other cancers. Focal amplifications of *NOTCH2* and *NOTCH3* were also observed, as were heterodimerization or extracellular domain mutations at lower incidence. Mutations and amplifications often activated the Notch pathway as evidenced by increased expression of canonical Notch target genes, and functional mutations were significantly enriched in the triple-negative breast cancer subtype (TNBC). PDX models were also identified that harbored PEST domain mutations, and these models were highly sensitive to PF-03084014.

Conclusions: This work suggests that Notch-altered breast cancer constitutes a *bona fide* oncogenic driver segment with the most common alteration being PEST domain mutations present in multiple Notch receptors. Importantly, functional studies suggest that this newly identified class can be targeted with Notch inhibitors, including GSIs. *Clin Cancer Res; 21(6); 1487–96.* ©*2015 AACR.*

Introduction

The Notch pathway is a highly conserved developmental pathway responsible for a variety of cell fate decisions (1–3). The pathway is activated during normal breast development, and has been implicated as a key driver in breast cancer (4–7). This has motivated the development of Notch inhibitors, including gamma secretase inhibitors (GSI), as the gamma secretase (GS) complex is required to cleave and activate all four Notch receptors (8). However, pinpointing where and how this complex pathway that has redundancy at several nodes is activated and identifying robust biomarkers of response represent a critical gap. Integrated omic datasets have recently been generated on hundreds of human tumors and relevant preclinical models, which now provide an opportunity to explore this question in detail. Within breast cancer, there is an urgent need to identify new therapeutic strategies for triple-negative breast cancer (TNBC) in particular, which is associated with a poor prognosis, lacks effective therapies, and does not have a well-established catalog of oncogenic drivers (9).

Notch is normally cleaved at the S1 site while trafficking in the Golgi and forms a bipartite receptor held together by noncovalent interactions within the heterodimerization (HD) domain. This domain is close to the membrane on the extracellular side of the cell and is flanked by site2 (S2) toward the C-terminus and a negative regulatory region (NRR) toward the N-terminus. In the unstimulated state, the NRR prevents access to and cleavage of the S2 site by an ADAM metalloprotease. Upon binding by a ligand expressed on an adjacent cell, a conformational change of the NRR exposes the S2 site, thus allowing its cleavage. The GS complex then mediates S3 cleavage within the transmembrane domain liberating the Notch intracellular domain (NICD), which translocates to the nucleus and regulates the transcription of target genes. An important mechanism of NICD regulation is protein turnover. It is normally degraded quickly due to the PEST domain located at the C-terminus (1, 10).

[1]Oncology Research Unit, Pfizer Global Research and Development, La Jolla, San Diego, California. [2]External Research Solutions, Pfizer Global Research and Development, La Jolla, San Diego, California.

Note: Supplementary data for this article are available at Clinical Cancer Research Online (http://clincancerres.aacrjournals.org/).

Current address for J. Christensen: Mirati Therapeutics Inc., San Diego, California.

Corresponding Author: Peter Olson, Oncology Research Unit, Pfizer, Inc., 10724 Science Center Drive, La Jolla, CA, 92122. Phone: 858-526-4995; Fax: 858-622-5999; E-mail: peter.olson@pfizer.com

doi: 10.1158/1078-0432.CCR-14-1348

Translational Relevance

Although the Notch pathway is reportedly activated in breast cancer, the molecular mechanisms leading to its aberrant activation are poorly understood, hampering the clinical development of Notch inhibitors. In this study, we demonstrate that the Notch pathway is activated via multiple mutational mechanisms primarily involving the PEST domain of NOTCH1, NOTCH2, and NOTCH3. Collectively, approximately 13% of triple-negative breast cancer exhibits a genetic alteration coupled with pathway upregulation, and these alterations may serve as biomarkers to identify patients most likely to respond to Notch inhibitors.

There is a growing list of mechanisms whereby Notch is activated by mutation or complex genetic rearrangements in cancer and human diseases. In T-cell acute lymphoblastic leukemia (T-ALL), translocations that remove a large portion of the extracellular domain (ECD) and heterodimerization domain mutations involving *NOTCH1* disrupt the normal function of the ECD/NRR and effectively lead to ligand-independent Notch activation (11, 12). Inactivating PEST domain mutations in *NOTCH1* that increase NICD1 half-life and Notch signaling are also frequently observed in T-ALL as well as chronic lymphocytic leukemia, splenic marginal zone lymphoma (SMZL), and mantle cell lymphoma (13–15). Similar *NOTCH2* PEST domain mutations are present in diffuse large B-cell lymphoma (DLBCL), SMZL, and Hadju–Cheney syndrome (16–20). More recently, chromosomal rearrangements involving *NOTCH1* and *NOTCH2* were identified in breast cancers (21). The common feature across the genomic rearrangements that were shown to activate Notch signaling was the removal of a large portion of the ECD leading to ligand-independent activation, which is reminiscent of translocations and heterodimerization domain mutations in T-ALL. However, mutations or rearrangements involving the PEST domain have not been previously characterized in breast cancer.

Materials and Methods

Cell lines and antibodies

All cell lines were obtained from the ATCC before 2009 (over 5 years ago, exact date not known). The HCC1599 cell line was short tandem repeat (STR) authenticated by the authors (May 2013) using the StemElite assay (Promega) at the University of Arizona Research Laboratory. The other cell lines used in this study were not STR authenticated as most of the samples were from older studies. The HCC1599 and HPB-ALL cells were grown in RPMI-1640 medium and supplemented with 10% FBS, 50 IU/mL penicillin/0.05 mg/mL streptomycin. The remaining cell lines were grown in media recommended by the suppliers with supplements, including HEPES buffer, sodium pyruvate, nonessential amino acids, penicillin–streptomycin, ITS, and glutamine.

The primary antibodies used were anti-NICD1 (CST #4147), anti-Notch1 (CST #3608), and anti-GAPDH (CST #2118) antibodies (Cell Signaling Technology).

In vivo studies

All in house *in vivo* studies were conducted in compliance with the Guide for Care and Use of Laboratory Animals and were approved by the Pfizer Global Research and Development Institutional Animal Care and Use committee. The authorization to use animals in the CERFE facilities at XenTech for the HBCx PDX model was obtained by The Direction des Services Vétérinaires, Ministère de l'Agriculture et de la Pêche, France (agreement no. B-91-228-107). The animal care and housing were in accordance with European Convention n° STE123. All experiments were performed in accordance with French legislation concerning the protection of laboratory animals, and in accordance with a currently valid license for experiments on vertebrate animals, issued by the French Ministry for Agriculture and Fisheries to Dr. Truong-An Tran, Study Director, Xentech (no. A 91-541 dated December 21, 2010; validity, 5 years). Tumor-bearing athymic nude mice were dosed twice daily at 140 mg/kg on a 12-day on, 4-day off schedule for two cycles. The MAXF1162 model was run at Oncotest, and all experiments were approved by the local authorities and were conducted according to all applicable international, national, and local laws and guidelines. Tumor-bearing nude mice were dosed twice daily at 140 mg/kg on a 10-day on, 4-day off schedule for three cycles. The AA1077 patient-derived and HCC1599 cell line xenograft models were run at Pfizer in SCID-Bg mice. Mice were dosed at 110 mg/kg twice daily for 9 days (AA1077) or at 120 mg/kg twice daily for 12 days (HCC1599). To evaluate efficacy, mice with palpable tumor sizes were randomly assigned to different groups, and the mean value of the tumor size was matched between the groups. Differences between the vehicle- and PF-03084014–treated groups were statistically significant by the Student *t* test. The percentage of tumor regression was calculated using the following formula $100 \times [1 - (\text{treated final volume}/\text{treated initial volume})]$ and the percentage of tumor growth inhibition was calculated using the following formula $100 \times [1 - (\text{treated final volume} - \text{treated initial volume})/(\text{vehicle final volume} - \text{vehicle initial volume})]$. For pharmacodynamic studies, tumor-bearing mice received 100 to 140 mg/kg PF-03084014 twice daily for 2 days before terminal collection. Some pharmacodynamic groups received one dose on the second day. The tumors were harvested 4 to 6 hours after the last dose, snap frozen and pulverized in a liquid nitrogen–cooled mortar before analysis.

DNA/RNA analysis

Genomic DNA and total RNA were prepared from cell pellet or frozen tumor tissue with the Qiagen DNeasy Blood and Tissue Kit (Cat. #69504) and the Qiagen RNeasy Mini Kit (Cat. 74104), following the manufacturer's protocol. Junction PCR was then performed to verify the break point of genomic DNA. Primer sequence for each particular sample is listed in the Supplementary Material. Total RNA were subjected to direct Quantitative RT-PCR (see below), or treated with calf intestinal phosphatase (CIP) and tobacco acidic pyrophosphatase (TAP), and then reverse transcribed to amplify the 5′ end messenger RNA sequence of *NOTCH1* in HCC1599. CIP and TAP were included in the FirstChoice RLM-RACE Kit from Life Technologies (cat. no. AM1700).

Transcriptomic sequencing (RNA-seq) of PDX models

RNA-seq was performed on PDX models with 100 bp (base pair) paired-end reads. Raw RNA-seq reads were filtered using Xenome (22) to remove potential reads from contaminating mouse cells. Non-mouse reads were then aligned to human

reference genome using TopHat2 (23). About 226.2, 253.9 and 298.3 million mapped reads were generated for HBCx14, AA1077, and MAXF1162, respectively.

TCGA data acquisition

Tier-2 mutation, somatic copy number, and mRNA expression data (RNA Seq V2 RSEM) from The Cancer Genome Atlas (TCGA) invasive breast carcinoma cohort were obtained from the TCGA data portal and Memorial Sloan Kettering Cancer Center's cBio portal (24). Raw Affymetrix SNP 6.0 array data were also downloaded from the TCGA data portal. Prealigned RNA-seq data (in BAM format) were downloaded via The Cancer Genomics Hub (25), dbGaP accession number PHS000178, version phs000178.v8.p7. A total of 956 tumors with complete mutation, copy-number, and gene-expression data were analyzed (Supplementary Table S1).

Gene-expression Analysis

Gene-expression profiles of the external PDX panel were generated using Affymetrix U133Plus2 arrays. CEL files were provided by the vendor (Xentech). Raw intensity data were processed by GC Robust Multiarray average background adjustment, quantile normalization, and median-polish summarization to generate the probe-level data in R. Normalized probe level data were further summarized into gene level using the GSEA CollapseDataset function.

Differential expression analysis of the Notch pathway genes in the TCGA breast cancer cohort were performed on the RNA-seq based Transcript per million metric from the RSEM results provided in the TCGA tier-3 data. Of the 130 TNBC tumors included in this cohort, 21 were selected as Notch altered that include patients with simple mutations or complex alterations in the heterodimerization or PEST domain of *NOTCH1*, *NOTCH2*, or *NOTCH3*, and those with focal amplification of *NOTCH2* or *NOTCH3* (inferred copy number >4). The Notch-nonaltered group included 50 TNBC tumors with no mutation, nor alteration, nor amplification (inferred copy number <2.5) in all Notch receptors. Note, that we did not include in this analysis TNBC tumors that harbor mutations or alterations in non-hotspot regions, and those with mild or broad copy-number gains, as they represent a "gray zone" that may blur the signal differentiating the two groups. Differential expression was calculated using a two-sample *t* test. Multiple hypothesis testing was controlled by FDR using the Benjamini–Hochberg method.

Nanostring Analysis

Nanostring technology (26) was used to measure the RNA transcript levels using the nCounter assay according to the manufacturer's recommended protocols. Briefly, transcript-specific capture and detection probes were designed and manufactured by the Nanostring Technologies and 100 ng of total RNA was hybridized to nCounter probe sets for 16 hours at 65°C. Samples were processed using an automated nCounter Sample Prep Station (NanoString Technologies, Inc.). Cartridges containing immobilized and aligned reporter complex were subsequently imaged and counted on an nCounter Digital Analyzer (NanoString Technologies, Inc.) set at 1,155 fields of view. Reporter counts were analyzed and normalized using NanoString's nSolver analysis software version 1.

Quantitative RT-PCR

Total RNA was isolated using the miRNeasy Mini Kit (Qiagen). Two micrograms of RNA per reaction was used to generate cDNA using the High Capacity cDNA Reverse Transcription Kit (Life Technology). Q-PCR was performed in triplicate by using ABI PRISM 7900HT Sequence Detection System with Taqman Universal PCR Master Mix (Life Technology). Primer/probes for Hes4, Hey1, Hey2, HeyL, Myc, NRARP, CCND1, and Notch3 were purchased from Life Technology. The expression level was normalized to GAPDH. Data normalized using hypoxanthine-guanine phosphoribosyltransferase and peptidylprolyl isomerase E yielded similar results.

Results

Identification of Notch receptor mutations and focal amplifications in the TCGA breast cancer dataset

To identify potential patient selection biomarkers for the GSI PF-03084014, we mined the TCGA breast cancer data for mutations and alterations involving Notch receptors (27). A number of mutations were reported by the standard TCGA pipeline or discovered internally in each receptor (Supplementary Figs. S1 and S2 and Supplementary Table S1). Of the 956 tumor samples analyzed with complete gene expression, copy-number, and mutation data, there were 42 mutations in *NOTCH1*, *NOTCH2*, or *NOTCH3*, 25 of which either clustered in the heterodimerization domain or led to a disruption of the PEST domain (Fig. 1A and Table 1). The PEST domain is a negative regulatory domain that is responsible for degrading the active NICD and, when disrupted, leads to an increase in the NICD half-life. Although PEST domain mutations in Notch are established oncogenic events in leukemias and lymphomas, they have not been characterized in breast cancer. The majority of PEST domain mutations were nonsense mutations or frameshifting indels, and were therefore predicted to truncate the normal protein sequence. The heterodimerization mutations on the other hand, occurred at highly conserved amino acid residues (28). Similar mutations are present in *NOTCH1* in T-ALL and activate Notch signaling (12). Although no mutations in this cohort were recurrent, several other mutations disrupted the protein at the same amino acid location as in other established Notch-driven cancers as well as Hadju–Cheney syndrome, a genetic disorder characterized by pathway-activating NOTCH2 PEST domain mutations (Table 1).

More complex structural variants were not provided by the standard TCGA pipelines. We therefore obtained the prealigned RNA-seq data from the TCGA breast cancer study and applied a suite of in-house algorithms, collectively called TopNotch, that are based on a local, *de novo* transcript assembly approach. This analysis identified six additional candidate alterations in five tumors predicted to activate the Notch pathway. Four alterations disrupted the PEST domains in *NOTCH1*, *NOTCH2*, or *NOTCH3* (Table 1, Fig. 1A; Supplementary Fig. S3). In terms of molecular mechanisms, three tumors harbored large deletions whereas one tumor harbored a translocation, all of which were predicted to remove the entire PEST domain (Table 1). One tumor harbored both a large PEST domain–disrupting deletion as well as a fusion with the *BRD4* gene in which exons 26-33 of *NOTCH3* (which encode NICD3) were fused downstream of exon 1 of a noncanonical *BRD4* transcript (Ensembl transcript ID: ENST00000360016). The fusion was predicted to lack the entire NOTCH3 ECD and produce an in-frame NICD3 with an

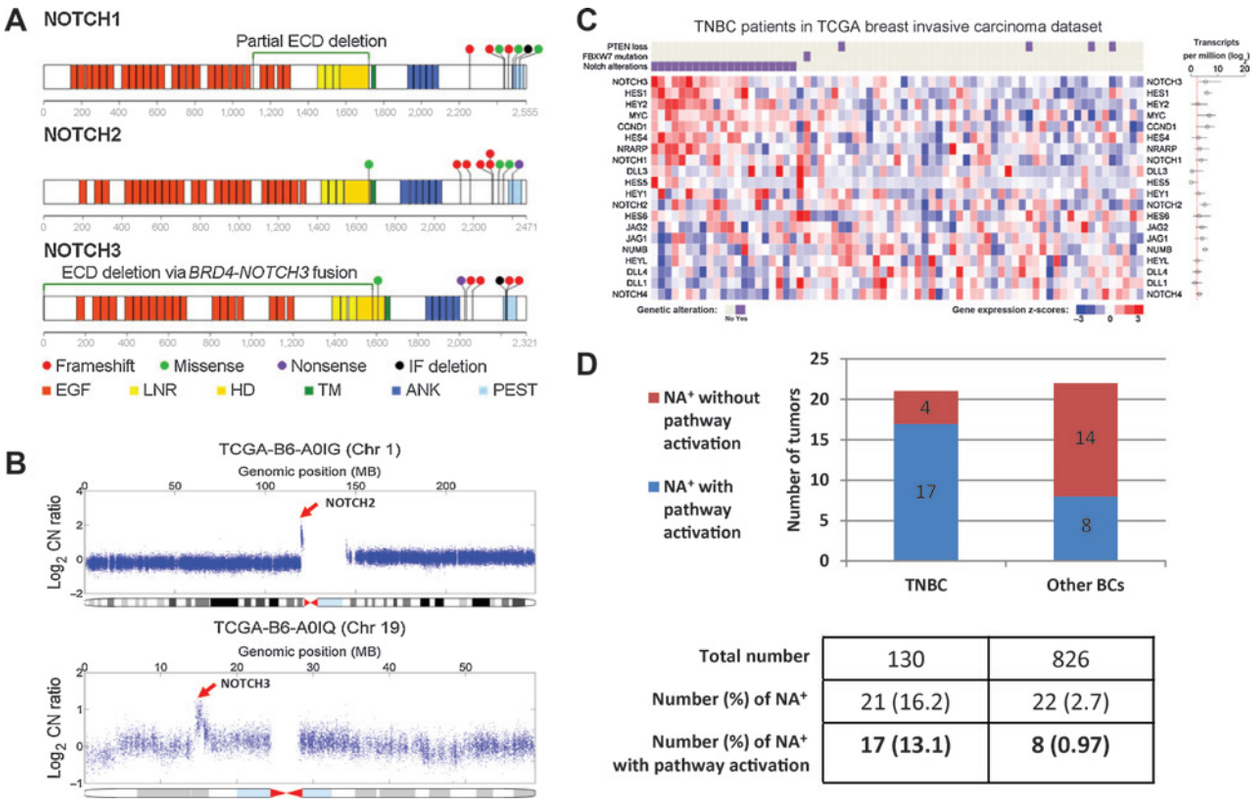

Figure 1.
Notch receptor mutations and focal amplifications in TCGA invasive breast cancer dataset exhibit pathway activation and are enriched in the triple-negative subtype. A, lollipop graph depicting simple mutations and complex alterations in *NOTCH1*, *2*, and *3* in the TCGA dataset clustered in or near the heterodimerization or PEST domains. The green dotted line indicates in-frame deletion (*NOTCH1)* or in-frame fusion (*BRD4–NOTCH3*), both of which are predicted to produce the NICD. Protein domains were obtained via a Pfam search (http://pfam.sanger.ac.uk/search) of the wt protein sequences. B, examples of TCGA tumors harboring focal amplifications of *NOTCH2* (top) or *NOTCH3* (bottom) copy-number (CN) ratio in $\log_2$ were calculated using data from the matched normal sample as reference. C, expression heatmap of Notch pathway genes in 21 Notch–altered TN tumors compared with 50 nonaltered TN tumors. See Materials and Methods for the selection of the two groups. Unscaled expression was shown to the right of the heatmap in which the circle indicates median expression and the line indicates the range of expression. The dotted red line indicates background expression level. D, Notch-altered tumors are enriched in TNBC and Notch-altered TNBC tumors are more likely to exhibit increased Notch pathway activity. BCs, breast cancers; NA, Notch altered.

intact GS site. Furthermore, we identified a tumor harboring a deletion of exons 21-27 in *NOTCH1*, which removes the NRR and heterodimerization domain. The PEST domain breakpoints identified from this analysis were further validated in the whole-exome sequencing data from the same patients because they were all located within the last exon of the Notch genes, including the matched normal samples to confirm their somatic status (see Materials and Methods; Supplementary Figs. S4–S6 and Supplementary Table S2).

We also analyzed the somatic copy-number alteration data for amplifications of Notch receptors and found a number of tumors with focal amplification of *NOTCH2* or *NOTCH3* (Fig 1B; Supplementary Fig. S1 and Supplementary Table S1). Focal amplification often led to overexpression of the receptor. Notably, similar to mutational patterns observed in other well-established oncogenic drivers, 37% of Notch mutations co-occurred with copy-number gain >3 at the locus (Table 1). Furthermore, 67% of the mutations exhibited very high expression of the Notch receptor (93rd percentile or greater), including all but one of the mutations that were coincident with copy-number gain. The mutation and expression pattern is most striking for *NOTCH3* in which of seven mutated tumor samples, four exhibit copy-number gain, two of which are focal, and all have either 97th or 99th percentile expression of *NOTCH3*. In contrast with *NOTCH1*, *NOTCH2*, and *NOTCH3*, no compelling mutations or amplifications were found in *NOTCH4* (Supplementary Fig. S2). In summary, we identified 43 breast cancers in the TCGA cohort that carry either somatic mutations in a hotspot domain (ECD/HD or PEST) of *NOTCH1-3*, or somatic focal amplification of *NOTCH2* or *NOTCH3* with concomitant increase in receptor expression (collectively referred to as "Notch altered" hereafter). Our analysis demonstrates a broad spectrum of potentially activating genetic alterations in Notch receptors is present in breast cancer, most often involving the PEST domain.

Notch-mutant and -amplified cancers are associated with the triple-negative subtype and pathway activation

To determine whether these potentially activating Notch alterations were associated with a breast cancer subtype, TCGA data were analyzed for Notch, ESR1, PGR, and ERBB2 status. Of the 956 tumor samples analyzed, 130 (or 13.6%) were determined to be TNBC (see Materials and Methods). Strikingly, 21 of the 43 Notch-altered breast cancers are TNBCs (a 3.6-fold enrichment, $P = 6.89E{-}6$ by Fisher exact test, Table 1 and Fig. 1D). This strong

Table 1. *NOTCH1*, *NOTCH2*, and *NOTCH3* hotspot mutations in TCGA breast tumors

TCGA ID	Notch	AA change	HD or PEST	Subtype	Hes4/ Hey2	Copy-number; focal (Y/N)	Rec exp percent	AA mutated in cancer/HCS
BH-A1FC	Notch1	V1110-S1723 IF del (exon 21-27 del)	HD	TNBC	Yes	4.6 (N)	99	BC (21)
A8-A08X	Notch1	A2256fs (translocation to chr14)	PEST	$ER^-/PR^-/HER2^+$	Yes	18.4 (N)	99	
EW-A1PH	Notch1	P2438fs (8 bp del)	PEST	TNBC	No	2.0	94	T-ALL (12)
AR-A254	Notch1	A2441T	PEST	$ER^+/PR^+/HER2^+$	No	2.0	40	T-ALL (35)
D8-A1XQ	Notch1	P2462fs (1 bp del)	PEST	TNBC	No	1.8	79	
BH-A18V	Notch1	Q2487L	PEST	TNBC	Yes	2.6	98	T-ALL, MCL (13, 36)
A2-A0T0	Notch1	S2499-F2554 IF del (168 bp del)	PEST	TNBC	Yes	1.3	93	
AR-A2LR	Notch1	S2523L	PEST	TNBC	No	1.6	96	
B6-A0X0	Notch2	V1666F	HD	ER^+/PR^+/HER2 unk	No	2.0	44	V1667I in SMZL (17)
B6-A3ZX	Notch2	L2135fs (2 bp del)	PEST	ER unk/$PR^-/HER2^-$	No	1.9	95	SMZL (15)
AO-A0J6	Notch2	T2186fs (62bp del)	PEST	TNBC	Yes	2.0	65	
B6-A0RE	Notch2	P2297fs (1 bp del)	PEST	TNBC	Yes	1.5	21	
E9-A244	Notch2	P2303fs (1 bp del)	PEST	TNBC	Yes	4.1 (N)	97	SMZL (17)
E9-A227	Notch2	P2303fs (1 bp ins)	PEST	$ER^+/PR^+/HER2^-$	No	2.0	54	SMZL (17)
AC-A23H	Notch2	A2331S	PEST	$ER^+/PR^-/HER2^+$	No	2.0	63	
A8-A0A6	Notch2	T2355P	PEST	$ER^+/PR^+/HER2^-$	No	24 (Y)	99	
EW-A1P8	Notch2	R2400*	PEST	TNBC	Yes	3.9 (N)	52	DLBCL, SMZL, HCS (15, 17, 18, 20)
AN-A0AR	Notch3	BRD4 fusion-M1583 and P2067fs (1326 bp del)	HD PEST	TNBC	Yes	0.9	97	
A2-A0SX	Notch3	A1608T	HD	TNBC	Yes	3.1 (N)	99	
B6-A0IQ	Notch3	Q2026*	PEST	TNBC	Yes	19.8 (Y)	99	
BH-A18G	Notch3	P2034fs (1 bp ins)	PEST	TNBC	Yes	2.0	97	
BH-A5IZ	Notch3	G2225del (3 bp del)	PEST	ER unk/$PR^-/HER2^-$	Yes	2.3	99	
BH-A0B9	Notch3	H2227fs (2 bp del)	PEST	TNBC	Yes	3.8 (N)	99	
AQ-A54N	Notch3	P2231fs (1 bp ins)	PEST	TNBC	Yes	20 (Y)	99	

NOTE: Somatic *NOTCH1*, *NOTCH2*, and *NOTCH3* mutations and alterations in the heterodimerization and PEST domains identified in the TCGA invasive breast carcinoma cohort. For complex alterations, genomic changes are indicated in parentheses following the amino acid (AA) change (details can be found in Supplementary Fig. S4). Hes4/Hey2 upregulation defined when either gene is expressed 2-fold above median expression across the cohort.
Abbreviations: DLBCL, diffuse large B-cell lymphoma; FS, frame-shift; HCS, Hajdu-Cheney Syndrome; IF, in-frame; MCL, mantle cell lymphoma; Rec exp percent, receptor expression percentile; SMZL, splenic marginal zone lymphoma; T-ALL, T-cell acute lymphocytic leukemia.

enrichment and the high unmet medical need in TNBC prompted us to focus on our subsequent analyses in this subtype. To determine whether Notch alteration resulted in increased Notch pathway activity, we compared Notch pathway gene expression in the 21 Notch–altered triple-negative tumors with Notch wild-type (wt) triple-negative tumors (Fig. 1C and Supplementary Table S3). Overall, a subset of Notch pathway and target genes, including *NOTCH3*, *HES1*, *HEY2*, *MYC*, *CCND1*, *HES4*, *NRARP*, and *NOTCH1*, exhibited significant overexpression (FDR<0.05) in the Notch-altered tumors, and were among the top 4% most upregulated genes in Notch-altered TNBCs when all genes were queried (Supplementary Table S3). One of the more provocative results in this dataset is the strong upregulation of the Notch pathway target genes *MYC* and *CCND1* in the Notch-altered breast tumors, providing insight into both the mechanism, whereby Notch activation may lead to an oncogenic phenotype, as well as how these classical breast cancer genes are, in fact, upregulated in this subset of breast tumors (29, 30). In addition, mutations in *PTEN* or *FBXW7*, which have been shown to confer resistance to a GSI in *NOTCH1*-mutant T-ALL (31, 32), do not co-occur with Notch alterations in this dataset.

As canonical Notch target genes *HES4* and *HEY2* were differentially expressed between the Notch-altered and wt triple-negative tumors, we used overexpression of one or both of these target genes as an indicator of Notch pathway activation (Supplementary Fig. S7). Of the 21 TNBCs with Notch alterations of interest, 17 showed evidence of Notch pathway activation. Outside TNBC, however, only eight of the 22 Notch-altered tumors showed evidence of pathway activation (Fig. 1D). This suggests that Notch alterations are more likely to be functionally relevant in the TNBC subtype, and we estimate that 13% of TNBC falls into this newly identified Notch-altered oncogenic driver class.

Patient-derived xenograft models harboring Notch receptor PEST mutations are sensitive to PF-03084014

To determine whether *in vivo* models harboring Notch receptor PEST domain mutations are sensitive to PF-03084014, we sequenced patient-derived xenograft (PDX) models using RNA-seq and whole-genome sequencing. We identified three PDX models all of which had distinct genomic rearrangements that truncated the PEST domain of *NOTCH1* or *NOTCH2* (Fig. 2A; Supplementary Figs. S8 and S9, and Supplementary Table S4). The MAXF1162 model harbored a translocation that fused the last exon of *NOTCH2* with intronic sequence from *NBPF8*, which disrupted the NOTCH2 PEST domain at amino acid 2320. Similar to several Notch receptor mutations in the TCGA data, this model also harbored a focal amplification of the *NOTCH2* locus (Supplementary Fig. S8). The AA1077 model harbored a transcript that fused part of the last exon of *NOTCH1* with intronic sequence from *NOTCH1* between exons 30 and 31, and disrupted the PEST domain at amino acid 2249. Using WGS data from this model, we confirmed that this was due to a tandem duplication between

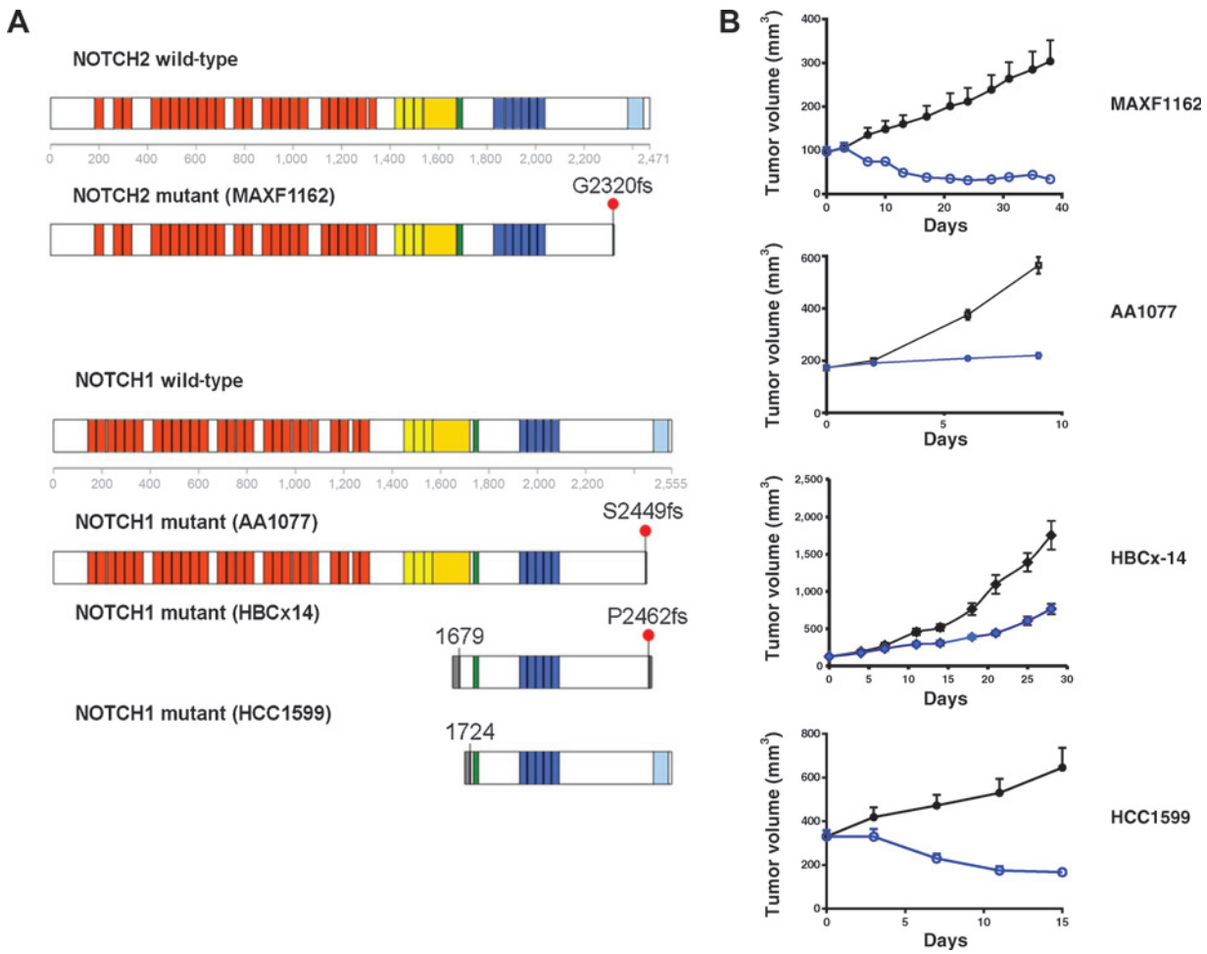

Figure 2.
Breast cancer models harboring Notch alterations are sensitive to PF-03084014. A, genomic alterations in Notch receptors in PDX models and the HCC1599 cell line model. The MAXF1162 model harbors a fusion that disrupts the *NOTCH2* PEST domain (red lollipop) as well as an amplification of the locus. The AA1077 model harbors a partial tandem duplication of *NOTCH1* that disrupts the *NOTCH1* PEST domain. The HBCx-14 model harbors an ECD deletion and a PEST domain frameshifting deletion in *NOTCH1*. The HCC1599 harbors an ECD deletion in *NOTCH1*. See Supplementary Figs. S8 and S9 for details of the alterations at genomic and transcript levels. B, Notch altered models are sensitive to PF-03084014. Data, average tumor volume + SEM. The MAXF1162 model exhibited 65% tumor regression, the AA1077 model exhibited 88% tumor growth inhibition, the HBCx-14 model exhibited 60% tumor growth inhibition, and the HCC1599 model exhibited 50% tumor regression. All models were statistically significant by the Student *t* test ($P < 0.05$).

intron 30 and exon 34 of *NOTCH1* (Supplementary Fig. S8). Finally, the HBCx-14 PDX model harbored a heterozygous 10 bp (frameshift) deletion in the PEST domain (disrupting the coding sequence beginning at amino acid 2462) and a homozygous ECD deletion (Supplementary Fig. S9 and Supplementary Table S4). Although the ECD was deleted, the GS site was still present in the mutated protein. All three models were highly sensitive to PF-03084014, including more than 50% tumor regression in the MAXF1162 model, which was similar to the *NOTCH1* ECD deleted HCC1599 cell line xenograft model previously known to be sensitive to GSI (Fig. 2B; refs. 33, 34). The MAXF1162 model was characterized as an HER2-amplified model, whereas the other models were triple negative.

To compare these responses in Notch-mutant models to Notch wt models, we analyzed a panel of eight xenograft models that were previously tested for sensitivity to PF-03084014 and for which we had treated and untreated samples that could be used for sequencing and pharmacodynamic gene-expression analyzes (Supplementary Fig. S10; ref. 33). No activating Notch hotspot domain alterations were found in RNAseq or whole-genome sequencing data from four PDX models [HBCx-5 (HER2$^+$), HBCx-17 (triple negative), HBCx-12B (triple negative), and AA0869 (triple negative)] and four cell line xenograft models [HCC1937 (triple negative), HCC1806 (triple negative), BT-474 (HER2$^+$), and MDA-MB-231 (triple negative)]. Responses in these Notch wt models were very heterogeneous ranging from little to no effect to slight tumor regression. On the other hand, all Notch-mutant models responded to PF-03084014, including greater than 50% tumor regression in two of four models. In summary, we identified mutations in PDX models representative of the TCGA mutations in terms of location, predicted functional consequence, spectrum of molecular mechanisms, and coincidence of multiple events. These data, therefore, confirm and extend our findings from the TCGA analysis and importantly, demonstrate that relevant preclinical models harboring Notch alterations are particularly sensitive to PF-03084014.

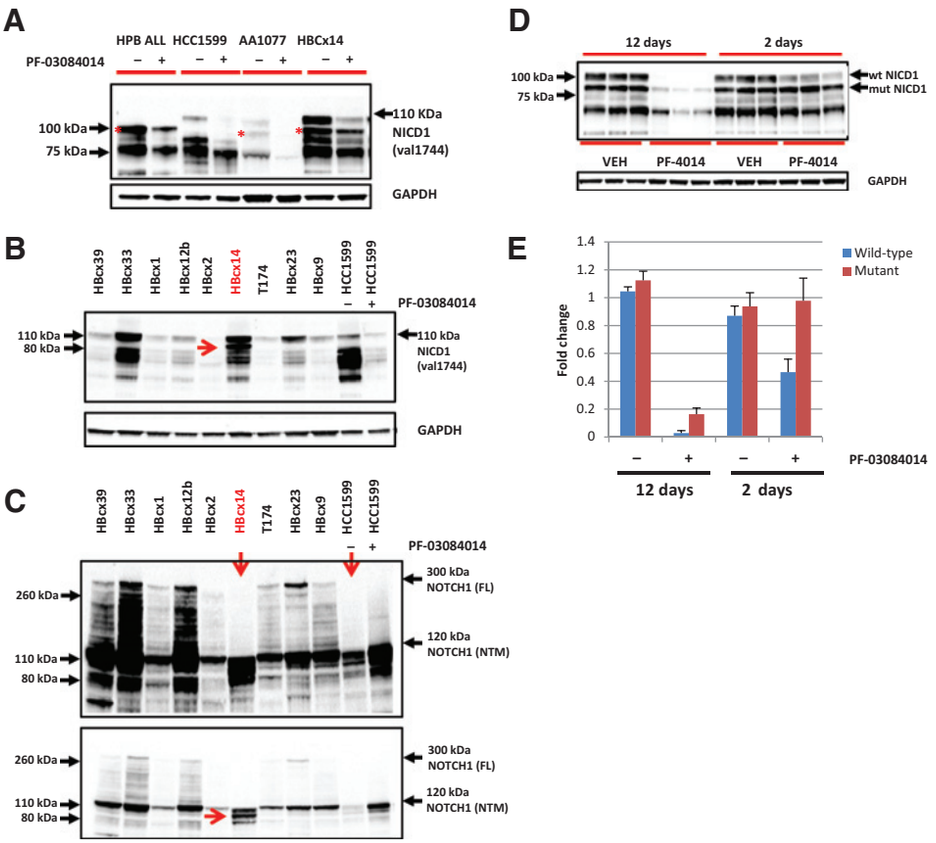

Figure 3.

NOTCH1 mutations alter full-length and NICD1 protein and NICD1 half-life. A, NICD1 Western blot analysis in Notch-altered models treated with or without PF-03084014. "*" indicates NICD1 species of lower molecular weight than wt NICD1. HPB-ALL is a T-ALL model that is known to generate an NICD1 species of lower molecular weight due to a PEST domain mutation. To better visualize the wt and mutant NICD1 bands in the newly discovered NOTCH1 mutant models, a 15-μg lysate was loaded for the HPB-ALL and HCC1599 models, 50 μg was loaded for the AA1077 model, and 30 μg was loaded for the HBCx-14 model. B, NICD1 Western blot analysis on the NOTCH1 PEST–truncated HBCx-14 model (lane 6) alongside a panel of lysates from TNBC PDX models from the same collection. The HCC1599 cell line xenograft model ± PF-03084014 for 2 days at 100 mg/kg twice daily was included as controls. A 50-μg lysate was loaded for all lysates except 25 μg for the HCC1599 lysates. The red arrow indicates the lower molecular weight NICD1 species in the HBCx-14 model. C, NOTCH1 Western blot analysis using an antibody that recognizes the NOTCH1 transmembrane and full-length species. Bottom, lighter exposure. The red arrows indicate the lower molecular weight species in the HBCx-14 model and the absence of detectable full-length protein in either the HBCx-14 model or the HCC1599 model. The same amount of lysate was loaded in a separate gel as in B on the same day; therefore, no additional loading control was included for this gel. D, 2 and 12 days treatment with PF-03084014 at 140 mg/kg twice daily. The PEST-mutated NICD1 was less diminished after drug treatment relative to the wt band. E, quantification of bands in D. Data, average band intensity ± SEM relative to 12 days vehicle and normalized to GAPDH. S3, cleavage site recognized by the GS complex; PEST, protein domain rich in proline (P), glutamic acid (E), serine (S), and threonine (T).

We next explored the functional consequences of the *NOTCH1* mutations on NICD1, the activated form of the receptor. Mutations that remove the ECD domain are predicted to result in ligand-independent activation of the receptor. Indeed, similar to the HCC1599 model, the HBCx-14 model exhibited robust NICD1 expression that was inhibited by PF-03084014 and lacked full-length NOTCH1 (Fig. 3A–C). On the other hand, PEST domain–truncating mutations in the AA1077 and HBCx-14 models produced a lower molecular weight NICD1 species as predicted. In contrast, NOTCH1 wt models did not exhibit strong expression of NICD1 nor were lower molecular weight species present (Supplementary Fig. S11).

We further explored the consequence of the PEST domain mutation in the HBCx-14 PDX model. In this model, a 2-day treatment with PF-03084014 dramatically reduced the wt NICD1 band. In contrast, the mutated NICD1 band appeared to be only slightly reduced (Fig. 3D). This is consistent with the prediction that PEST-mutant NICD1 has a longer half-life. To quantify this effect, we measured the average intensity of wt and mutated NICD1 bands in the HBCx-14 model from three animals treated for either 2 or 12 days with PF-03084014. Short-term treatment reduced the wt band to approximately 50% of untreated levels whereas the mutated band was not significantly reduced (Fig. 3D and E). In 12-day treated mice, wt NICD1 was reduced to less than 3% of untreated wt levels whereas mutant NICD1 was present at approximately 15% of untreated mutant levels. These data demonstrate that mutations truncating the PEST domain in breast cancer models can increase the protein half-life of NICD1.

Activating alterations in Notch receptors would be predicted to upregulate direct transcriptional targets of the pathway, including the Hes and Hey family transcription factors, similar to the TCGA gene-expression analysis. Indeed, in an initial survey of gene-

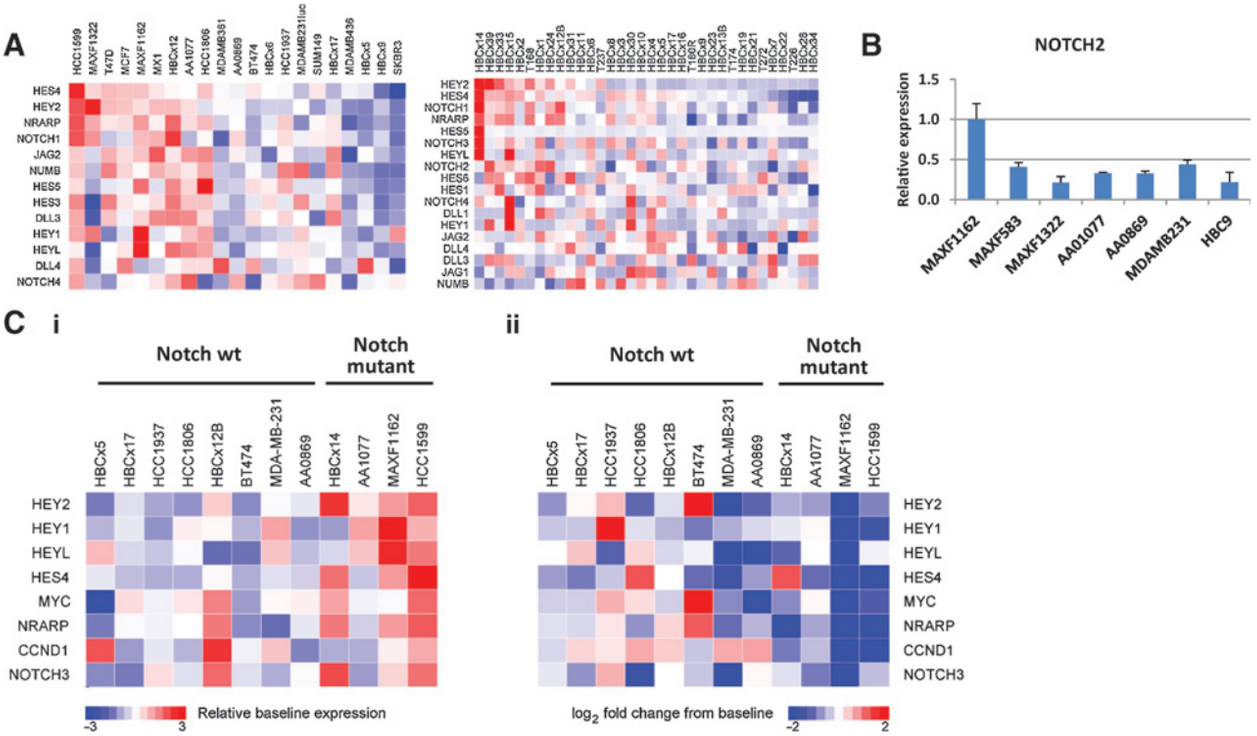

Figure 4.
Notch-mutant breast cancer models often exhibit increased Notch pathway expression sensitive to PF-03084014. A, models rank ordered from left to right using an *HES4*, *HEY2* two gene signature score across an internal *in vivo* (left) and an external PDX panel (right). B, relative *NOTCH2* expression normalized against β-actin across the panel of internal *in vivo* models. C, i, quantitative RT-PCR of key Notch target genes at baseline in Notch wt and Notch-altered models demonstrate Notch-altered models exhibit high level expression of one or more genes, the *HES* and *HEY* family genes in particular. C, ii, fold change from baseline following 2 days of treatment with PF-03084014. Notch target genes were consistently downregulated by PF-03084014 treatment in Notch-mutant models and were downregulated to a greater degree compared with Notch wt models. Nanostring digital gene-expression data were used for the internal *in vivo* model; Affymetrix microarray gene-expression data were used for the external PDX model panel; qRT-PCR data were used for C.

expression levels of Notch pathway genes across the panels of *in vivo* models, we observed strong overexpression of *HES4*, *HEY2*, *HEY1*, and/or *HEYL* in three of the four Notch-mutant models (Fig. 4A). The MAXF1162 and HBCx-14 models both harbored multiple genetic events in the altered Notch receptor, and in both cases the mutated receptor itself exhibited the highest mRNA expression among the panel of the xenograft screened (Fig 4A and B). We next used quantitative RT-PCR to analyze Notch target gene expression between Notch-mutated and Notch wt xenograft models treated with or without PF-03084014. Treatment with drug reduced the expression of nearly all Hes and Hey target genes in the Notch-altered models that exhibited strong overexpression at baseline demonstrating Notch alterations indeed drive the Notch pathway in these models and that PF-03084014 can effectively repress this hyperactivated transcriptional program (Fig. 4C and Supplementary Fig. S12). In addition, the Notch target genes *MYC*, *NRARP*, *CCND1*, and *NOTCH3* were also nearly always downregulated by PF-03084014 (Fig. 4C and Supplementary Fig. S13). In contrast, in Notch wt models, Notch target genes very rarely exhibited strong overexpression at baseline. Moreover, although treatment with PF-03084014 downregulated Notch target genes in some Notch wt models, the number of targets regulated by PF-03084014 and the magnitude of downregulation was less, on average, than in the Notch-altered models (Fig. 4C and Supplementary Figs. S12 and S13). Taken together, these functional studies in preclinical *in vivo* models demonstrate PEST domain mutations in Notch receptors activate the Notch pathway, confer sensitivity to PF-03084014, and provide strong rationale for a personalized medicine strategy for Notch inhibitors in Notch-altered TNBC.

Discussion

In this study, a broad spectrum of activating mutations were discovered in *NOTCH1*, *NOTCH2*, and *NOTCH3*, including missense mutations, nonsense mutations, small indels, large deletions, and chromosomal translocations that disrupt either the ECD/HD or PEST domains. This repertoire of mutational mechanisms involving the PEST domains is in contrast with the molecular mechanisms of previously known PEST domain mutations in leukemias and lymphomas that primarily consist of point mutations and small indels (13–15, 17–19). We also found evidence for heterodimerization or ECD mutations similar to what have been previously reported; however, these mutations appear to have a lower prevalence compared with mutations involving the PEST domain.

An interesting observation from this study is the nature of the Notch mutations and alterations. Typically, activating oncogenic mutations is restricted to a few hotspots within a gene, and inappropriately activate a signal transduction cascade: for example, mutations in *KRAS* at codons 12, 13 or 61, or the L858R mutation or exon 19 deletion of *EGFR*. Conversely, tumor-

suppressor genes such as *TP53* are often altered at multiple locations along the gene. Notch receptors are somewhat unique in that the PEST domains and ECD/HD, in essence, negatively regulate the active form of Notch, the NICD. Therefore, inactivation by mutation or deletion of either domain activates the Notch pathway.

The coincidence of mutations with amplification and overexpression of the Notch receptor is similar to other established oncogenes, and suggests that there is pressure to select for high levels of Notch pathway activity. Increased receptor expression may be important, given the unique mechanism of Notch activation, which lacks a true signal amplification step. GS cleavage generates the active NICD molecule, which directly translocates to the nucleus and activates a downstream transcriptional program. Therefore, the maximal activity of the pathway is directly linked to Notch receptor concentration. In the case of the MAXF1162 model that harbors a PEST domain mutation and focal amplification, the receptor amplification may be required to boost the baseline signaling, whereas the PEST domain mutation would be predicted to further increase the duration of the active Notch signal.

The number and complexity of Notch mutations may preclude a definitive immediate interpretation for every alteration observed in the TCGA breast cancer dataset. Reliable functional studies capable of measuring Notch pathway activation, transformation potential, and sensitivity to pathway inhibition will be required to better understand all of the mutations and alterations examined in this study. However, the observation that many of these mutations are recurrent in other cancers or diseases in which pathway activation is an established pathogenic event provides strong evidence that these alterations are operative in breast cancer. Moreover, the increased expression of Notch pathway target genes in Notch-altered human tumors and sensitivity to a GSI in Notch-altered preclinical models provide compelling evidence that many of these mutations are oncogenic.

This dataset is timely, as several Notch pathway inhibitors that target various points in the pathway are currently in early clinical development. Given the spectrum of Notch alterations observed, it should be anticipated that each drug will produce different responses depending on the nature of the mutations. For instance, inhibitory antibodies against Notch receptors will likely only work against tumors in which the domain recognized by the antibody remains intact after the genomic alteration. On the other hand, GSIs should inhibit activating Notch alterations in which the GS cleavage site remains intact, which includes nearly all of the activating Notch alterations described in breast cancer thus far. Collectively, these data suggest an appreciable fraction of patients with TNBC harbor oncogenic Notch alterations that may be effectively treated with targeted inhibitors.

Disclosure of Potential Conflicts of Interest

K. Ching, P. Rejto, J. Christensen, and P. Olson have ownership interest in Pfizer. No potential conflicts of interest were reported by the other authors.

Authors' Contributions

Conception and design: K. Wang, J. Christensen, P. Olson
Development of methodology: K. Wang, D. Li, X. Zheng, S. Shi, X. Li, P. Olson
Acquisition of data (provided animals, acquired and managed patients, provided facilities, etc.): K. Wang, Q. Zhang, D. Li, C. Zhang, X. Zheng, M. Ozeck, X. Li, H. Wang, P. Olson
Analysis and interpretation of data (e.g., statistical analysis, biostatistics, computational analysis): K. Wang, Q. Zhang, K. Ching, X. Zheng, M. Ozeck, P. Rejto, J. Christensen, P. Olson
Writing, review, and/or revision of the manuscript: K. Wang, P. Rejto, P. Olson
Administrative, technical, or material support (i.e., reporting or organizing data, constructing databases): K. Wang, K. Ching, M. Ozeck, P. Olson
Study supervision: K. Wang, C. Zhang, S. Shi, P. Rejto, J. Christensen, P. Olson

Acknowledgments

The authors thank Enhong Chen and Maruja Lira for technical assistance. The authors thank Chih-Hao Lee (Harvard School of Public Health) for critical reading of the article. The results published here are, in part, based upon data generated by TCGA pilot project established by the NCI and NHGRI, available as dbGaP accession number PHS000178, version phs000178.v8.p7. Information about TCGA and the investigators and institutions that constitute the TCGA research network can be found at http://cancergenome.nih.gov/.

The costs of publication of this article were defrayed in part by the payment of page charges. This article must therefore be hereby marked advertisement in accordance with 18 U.S.C. Section 1734 solely to indicate this fact.

Received May 27, 2014; revised November 20, 2014; accepted December 23, 2014; published OnlineFirst January 6, 2015.

References

1. Andersson ER, Sandberg R, Lendahl U. Notch signaling: simplicity in design, versatility in function. Development 2011;138:3593–612.
2. Artavanis-Tsakonas S, Matsuno K, Fortini ME. Notch signaling. Science 1995;268:225–32.
3. Kopan R, Ilagan MX. The canonical Notch signaling pathway: unfolding the activation mechanism. Cell 2009;137:216–33.
4. Callahan R, Egan SE. Notch signaling in mammary development and oncogenesis. J Mammary Gland Biol Neoplasia 2004;9:145–63.
5. Farnie G, Clarke RB. Mammary stem cells and breast cancer—role of Notch signalling. Stem Cell Rev 2007;3:169–75.
6. Guo S, Liu M, Gonzalez-Perez RR. Role of Notch and its oncogenic signaling crosstalk in breast cancer. Biochim Biophys Acta 2011;1815:197–213.
7. Buono KD, Robinson GW, Martin C, Shi S, Stanley P, Tanigaki K, et al. The canonical Notch/RBP-J signaling pathway controls the balance of cell lineages in mammary epithelium during pregnancy. Dev Biol 2006;293:565–80.
8. Wei P, Walls M, Qiu M, Ding R, Denlinger RH, Wong A, et al. Evaluation of selective gamma-secretase inhibitor PF-03084014 for its antitumor efficacy and gastrointestinal safety to guide optimal clinical trial design. Mol Cancer Ther 2010;9:1618–28.
9. Foulkes WD, Smith IE, Reis-Filho JS. Triple-negative breast cancer. N Engl J Med 2010;363:1938–48.
10. Fortini ME. Gamma-secretase-mediated proteolysis in cell-surface-receptor signalling. Nature reviews Mol Cell Biol 2002;3:673–84.
11. Ellisen LW, Bird J, West DC, Soreng AL, Reynolds TC, Smith SD, et al. TAN-1, the human homolog of the Drosophila notch gene, is broken by chromosomal translocations in T lymphoblastic neoplasms. Cell 1991;66:649–61.
12. Weng AP, Ferrando AA, Lee W, Morris JPt, Silverman LB, Sanchez-Irizarry C, et al. Activating mutations of NOTCH1 in human T-cell acute lymphoblastic leukemia. Science 2004;306:269–71.
13. Kridel R, Meissner B, Rogic S, Boyle M, Telenius A, Woolcock B, et al. Whole transcriptome sequencing reveals recurrent NOTCH1 mutations in mantle cell lymphoma. Blood 2012;119:1963–71.
14. Puente XS, Pinyol M, Quesada V, Conde L, Ordonez GR, Villamor N, et al. Whole-genome sequencing identifies recurrent mutations in chronic lymphocytic leukaemia. Nature 2011;475:101–5.
15. Rossi D, Trifonov V, Fangazio M, Bruscaggin A, Rasi S, Spina V, et al. The coding genome of splenic marginal zone lymphoma: activation of NOTCH2 and other pathways regulating marginal zone development. J Exp Med 2012;209:1537–51.

16. Isidor B, Lindenbaum P, Pichon O, Bezieau S, Dina C, Jacquemont S, et al. Truncating mutations in the last exon of NOTCH2 cause a rare skeletal disorder with osteoporosis. Nat Genet 2011;43:306–8.
17. Kiel MJ, Velusamy T, Betz BL, Zhao L, Weigelin HG, Chiang MY, et al. Whole-genome sequencing identifies recurrent somatic NOTCH2 mutations in splenic marginal zone lymphoma. J Exp Med 2012;209:1553–65.
18. Lee SY, Kumano K, Nakazaki K, Sanada M, Matsumoto A, Yamamoto G, et al. Gain-of-function mutations and copy number increases of Notch2 in diffuse large B-cell lymphoma. Cancer Sci 2009;100:920–6.
19. Lohr JG, Stojanov P, Lawrence MS, Auclair D, Chapuy B, Sougnez C, et al. Discovery and prioritization of somatic mutations in diffuse large B-cell lymphoma (DLBCL) by whole-exome sequencing. Proc Natl Acad Sci U S A 2012;109:3879–84.
20. Simpson MA, Irving MD, Asilmaz E, Gray MJ, Dafou D, Elmslie FV, et al. Mutations in NOTCH2 cause Hajdu-Cheney syndrome, a disorder of severe and progressive bone loss. Nat Genet 2011;43:303–5.
21. Robinson DR, Kalyana-Sundaram S, Wu YM, Shankar S, Cao X, Ateeq B, et al. Functionally recurrent rearrangements of the MAST kinase and Notch gene families in breast cancer. Nat Med 2011;17:1646–51.
22. Conway T, Wazny J, Bromage A, Tymms M, Sooraj D, Williams ED, et al. Xenome—a tool for classifying reads from xenograft samples. Bioinformatics 2012;28:i172–8.
23. Trapnell C, Pachter L, Salzberg SL. TopHat: discovering splice junctions with RNA-Seq. Bioinformatics 2009;25:1105–11.
24. Available from: http://www.cbioportal.org/public-portal/
25. Available from: https://cghub.ucsc.edu/
26. Geiss GK, Bumgarner RE, Birditt B, Dahl T, Dowidar N, Dunaway DL, et al. Direct multiplexed measurement of gene expression with color-coded probe pairs. Nat Biotechnol 2008;26:317–25.
27. Cancer Genome Atlas N. Comprehensive molecular portraits of human breast tumours. Nature 2012;490:61–70.
28. Malecki MJ, Sanchez-Irizarry C, Mitchell JL, Histen G, Xu ML, Aster JC, et al. Leukemia-associated mutations within the NOTCH1 heterodimerization domain fall into at least two distinct mechanistic classes. Mol Cell Biol 2006;26:4642–51.
29. Arnold A, Papanikolaou A. Cyclin D1 in breast cancer pathogenesis. J Clin Oncol 2005;23:4215–24.
30. Efstratiadis A, Szabolcs M, Klinakis A. Notch, Myc, and breast cancer. Cell Cycle 2007;6:418–29.
31. O'Neil J, Grim J, Strack P, Rao S, Tibbitts D, Winter C, et al. FBW7 mutations in leukemic cells mediate NOTCH pathway activation and resistance to gamma-secretase inhibitors. J Exp Med 2007;204:1813–24.
32. Palomero T, Sulis ML, Cortina M, Real PJ, Barnes K, Ciofani M, et al. Mutational loss of PTEN induces resistance to NOTCH1 inhibition in T-cell leukemia. Nat Med 2007;13:1203–10.
33. Zhang CC, Pavlicek A, Zhang Q, Lira ME, Painter CL, Yan Z, et al. Biomarker and pharmacologic evaluation of the gamma-secretase inhibitor PF-03084014 in breast cancer models. Clin Cancer Res 2012;18:5008–19.
34. Zhang CC, Yan Z, Zong Q, Fang DD, Painter C, Zhang Q, et al. Synergistic effect of the gamma-secretase inhibitor PF-03084014 and docetaxel in breast cancer models. Stem Cells Translational Med 2013;2:233–42.
35. Larson Gedman A, Chen Q, Kugel Desmoulin S, Ge Y, LaFiura K, Haska CL, et al. The impact of NOTCH1, FBW7 and PTEN mutations on prognosis and downstream signaling in pediatric T-cell acute lymphoblastic leukemia: a report from the Children's Oncology Group. Leukemia 2009;23:1417–25.
36. Breit S, Stanulla M, Flohr T, Schrappe M, Ludwig WD, Tolle G, et al. Activating NOTCH1 mutations predict favorable early treatment response and long-term outcome in childhood precursor T-cell lymphoblastic leukemia. Blood 2006;108:1151–7.